BULLETIN OF STOMATOLOGY AND MAXILLOFACIAL SURGERY Volume 21, Issue 7

DOI: 10.58240/1829006X-2025.21.7-213



ORIGINAL ARTICALE

CHARACTERIZATION TEST (FUNCTIONAL GROUPS, CRYSTAL STRUCTURE) OF FREEZE-DRIED BOVINE GRAFT WITH NANOFAT MIXTURE AS A CANDIDATE FOR GRAFT MATERIAL

Putri Putra Rimba¹, Lobredia Zarasade¹, Agus Santoso Budi¹, Atikah¹

¹ Department of Plastic, Reconstructive and Aesthetic Surgery, Faculty of Medicine, Airlangga University, Dr. Soetomo General Hospital, Surabaya, Indonesia.

*Corresponding Author: Putri Putra Rimba, Department of Plastic, Reconstructive and Aesthetic Surgery, Faculty of Medicine, Airlangga University, Dr. Soetomo General Hospital, Surabaya, Indonesia. Email: putriputra.r@gmail.com *Received:* JuL 10. 2025; Accepted: Aug 8, 2025; Published: Aug 17, 2025

ABSTRACT

This study aimed to evaluate the incidence of neurosensory disturbance (NSD) following two modifications of bilateral sagittal split mandibular osteotomy (BSSO)—low medial cut (Posnick modification) and high medial cut (standard)—in the immediate postoperative period and after a minimum follow-up of six months. Twenty patients with skeletal Class III deformity requiring mandibular setback were randomly divided into two equal groups. Subjective and objective testing for inferior alveolar nerve function was performed. The results showed that all patients (except four in the Posnick group) exhibited some degree of NSD immediately postoperatively. However, at the 6-month follow-up, a complete recovery of NSD was reported in 74% of the low medial cut group and 35% of the high medial cut group. The low medial cut (Posnick) osteotomy demonstrated a shorter average osteotomy duration (20.30 minutes) compared to the high medial cut (27.21 minutes) and allowed for better visualization of the inferior alveolar nerve with decreased medial dissection. The study concludes that the low medial cut (Posnick) SSO is a valuable osteotomy technique, offering shorter osteotomy duration, decreased incidence of bad split, and better neurosensory recovery in the extended follow-up period compared to the traditional BSSO.

Keywords: bone regeneration; bone scaffold; freeze-dried bovine bone; FTIR; hydroxyapatite; nanofat; XRD

INTRODUCTION

Approximately 40% of hard tissue damage in Indonesia is caused by trauma or bone cancer. Restorative efforts are often carried out through transplantation or implantation of bone grafts. Among the available options, autogenous bone grafts remain the gold standard for maxillofacial reconstruction due osteogenic, their osteoinductive, osteoconductive properties. However, the harvesting procedure for autografts poses several drawbacks, including additional surgical wounds, donor site pain, increased operative time. and potential complications.1

As alternatives, allografts and xenografts have been developed. Allografts are grafts obtained from other individuals, including cadavers or living donors with or without genetic relation. They offer osteoconductive and osteoinductive effects, eliminate the need for secondary surgical procedures at the recipient site, reduce operative time, and minimize bleeding and postoperative complications.

Nonetheless, allografts may still induce immune responses, carry a risk of infectious disease transmission, and are limited in availability.⁸

Xenografts, on the other hand, are derived from different species—commonly bovine or porcine. They are readily available in large quantities and act as effective osteoconductive scaffolds. However, they lack viable cells and do not participate directly in osteogenesis. One commonly used xenograft is freeze-dried bovine bone (FDBB), which maintains the mineral and porous structure of native bone and serves as a scaffold in bone regeneration procedures. In recent years, advances in tissue engineering have introduced the integration of mesenchymal stem cells (MSCs) with scaffold materials to promote osteointegration and healing. MSCs can be isolated from bone marrow, adipose tissue, periosteum, and umbilical cords. Studies have shown that combining MSCs with bone substitutes can enhance healing, especially in large bone defects.⁷

Among various MSC sources, adipose tissue has

Putri Putra Rimba, Lobredia Zarasade, Agus Santoso Budi, Atikah, Characterization Test (Functional Groups, Crystal Structure) of Freeze-Dried Bovine Graft with Nanofat Mixture as a Candidate for Graft Material. Bulletin of Stomatology and Maxillofacial Surgery.2025;21(7).213-218 doi:10.58240/1829006X-2025.21.7-213

emerged as a promising candidate due to its abundance and ease of harvesting. A recent innovation involves the emulsification and filtration of adipose tissue to produce nanofat, a fluid rich in adipose-derived stem cells (ADSCs), growth factors, extracellular matrix proteins, and lipids. Unlike microfat, nanofat lacks adipocytes and does not serve as a filler, but rather as a bioactive agent promoting regeneration through paracrine mechanisms.^{5,7}

Nanofat offers several advantages: regenerative capability, injectability, minimal immunogenicity, and ease of integration into various clinical applications, including skin rejuvenation, soft tissue repair, and more recently, bone regeneration. The technique was pioneered by Tonnard et al. (2013), who demonstrated improved skin quality after nanofat injection. Subsequent studies confirmed that nanofat contains a high concentration of stem cells and cytokines that stimulate osteoblast activity and bone formation.4,6,17

Further research by Bonomi et al. (2024) showed that combining nanofat with dermal substitutes enhanced vascularization and tissue integration in wound healing, without affecting biocompatibility.³ Based on these findings, we hypothesize that integrating nanofat with bone graft scaffolds could potentiate both osteogenic and angiogenic properties. However, to the best of our knowledge, such a combination has not been previously characterized using material analysis techniques.

Therefore, this study aims to evaluate the functional group and crystal structure characteristics of FDBB with nanofat mixtures using Fourier Transform Infrared Spectroscopy (FTIR) and X-Ray Diffraction (XRD). These analyses are crucial in determining whether the chemical composition and crystalline integrity of the scaffold are enhanced or disrupted by nanofat addition, thereby validating its potential as a novel graft material for bone defect reconstruction.

MATERIALS AND METHODS

This study was designed as a laboratory-based experimental research using a post-test only control group approach. Ethical approval was granted by the Research Ethics Committee of Airlangga University Hospital (Approval No. 093/KEP/2025), which reviewed and approved the protocol in accordance with the protection of human rights and the welfare of research participants.

The research aimed to evaluate the influence of nanofat addition on the chemical and structural properties of freeze-dried bovine bone (FDBB), with specific attention to functional group profiles and crystal structure. The independent variable in this study was the administration of nanofat in two volumes (1 cc and 2 cc) applied to 1 cm³ blocks of FDBB. The dependent variables were the functional group composition and crystalline structure of the samples, as assessed through Fourier Transform Infrared Spectroscopy (FTIR) and X-Ray Diffraction (XRD), respectively.

The FDBB samples were sourced from the Tissue Bank at Dr. Soetomo General Academic Hospital, Surabaya, Indonesia. These samples were processed from bovine femoral cancellous bone cut into $1\times1\times1$ cm blocks. The bone was chemically cleansed using 3% hydrogen peroxide, rinsed with sterile distilled water, freeze-dried to a moisture content below 10%, and finally sterilised via gamma irradiation. Each sample was weighed and placed in sterile petri dishes labelled according to group allocation: control (no nanofat), 1 cc nanofat, and 2 cc nanofat.

Nanofat was prepared from adipose tissue harvested from the lower abdominal region following infiltration with a modified Klein solution (lidocaine 800 mg/L and adrenaline 1:1,000,000). The tissue was aspirated using a 3 mm multi-port cannula with 1 mm side holes, washed with saline, and filtered through sterile nylon mesh (0.5 mm). Emulsification was conducted mechanically by passing the adipose tissue between two 10 cc syringes connected with Luer-lock connectors of progressively smaller diameters (2.4 mm, 1.4 mm, and 1.2 mm) for a minimum of 30 passes. The resulting emulsion was transferred into 1 cc syringes using a nanotransfer filter, yielding nanofat with particle sizes ranging from 400 to 600 µm. The nanofat was then dropwise applied onto the FDBB surfaces, allowing it to fully absorb until the surface appeared more yellowish in tone. Each sample was subsequently fixed using a graded ethanol series (50%, 70%, and 90%) for 10 minutes per concentration.

Characterisation of the samples involved two primary analytical techniques. FTIR was employed to evaluate the functional group composition. The spectra were recorded in the mid-infrared region (4000–450 cm⁻¹), focusing on the identification of typical bonerelated bands such as hydroxyl (–OH), aliphatic (–CH), carbonyl (C=O), amide I, and phosphate (PO₄³⁻). All FDBB samples, both untreated and nanofat-treated, demonstrated these characteristic bands. The addition of nanofat enhanced the expression of organic functional groups, particularly those related to proteins and lipids, without eliminating essential mineral components such as phosphate. This finding suggests that nanofat contributes to increased bioactive content while preserving the fundamental chemical integrity of the scaffold.

XRD analysis was conducted to assess the crystallographic structure of the samples. The diffraction patterns were recorded and interpreted based on the intensity and position of the peaks (2θ angles), allowing

the determination of crystal phases and degree of crystallinity. Both control and treated groups exhibited diffraction patterns consistent with the hydroxyapatite phase, indicating that nanofat did not interfere with the mineral lattice structure of FDBB.

This research was carried out at the Dental Research Center of the Faculty of Dental Medicine, Airlanga University, for sample preparation and fixation. FTIR and XRD analyses were conducted at Sepuluh Nopember Institute of Technology, Surabaya. The study was conducted over a period from April to May 2025. Data from both FTIR and XRD analyses were reported descriptively, highlighting the spectral and structural differences observed between groups.

RESULTS

The Fourier Transform Infrared Spectroscopy (FTIR)

analysis of freeze- dried bovine bone (FDBB) without nanofat exhibited characteristic absorption bands of natural bone tissue. A broad band between 3435-3786 cm⁻¹ indicated the presence of hydroxyl (OH) groups, originating from bound water or free hydroxyl groups within the mineral matrix. Aliphatic C–H stretching bands were observed at 2920 and 2854 cm⁻¹, attributed to residual protein or lipids. A strong absorption band at 1745 cm⁻¹ corresponded to carbonyl (C=O) stretching from ester or lipid residues. The amide I band at approximately 1650 cm⁻¹ represented the presence of collagen. Carboxylate groups (COO- bending) were also present at 1400–1460 cm⁻¹. Crucially, phosphate (PO₄³⁻) groups indicative of hydroxyapatite were observed at 1032–1090 cm⁻¹ (stretching), 875 cm⁻¹ (bending), and 560-600 cm⁻¹.

Table 1. FTIR interpretation of FDBB without nanofat (control)

-		* /
Standard Wavenumber (cm ⁻¹)		Observed Frequency (cm ⁻¹)
Hydroxyl (O-H Stretch)	3400 – 3700	3435 – 3786
Methyl C-H (CH ₂ , CH ₃)	2920 - 2850	2920 - 2854
Lipids/phospholipids (C=O ester)) 1740 – 1750	1745
Protein (collagen) (C=O amide I)	1650 – 1630	1639 – 1650
Carboxylic acid/collagen (COObending)	1450 – 1410	1400 – 1460
Phosphate (PO ₄ ³⁻) 600	1030 – 1090 / 8	875 / 560 – 1032 – 1090 / 875 / 560 – 600

The FTIR spectrum of FDBB mixed with 1 cc of nanofat showed an increase in intensity across several bands associated with organic compounds. Enhanced hydroxyl (OH) groups were evident between 3360–3490 cm⁻¹, likely derived from polar molecules in nanofat. Aliphatic C–H bands were visible at 2920 and 2852 cm⁻¹. A strong ester carbonyl (C=O) absorption at 1745 cm⁻¹, along with amide I at 1651 cm⁻¹, confirmed the presence of proteins and lipids. Carboxylate peaks at 1402–1462 cm⁻¹ and consistent phosphate bands confirmed the retention of bone mineral components.

Table 2. FTIR interpretation of FDBB with 1 cc nanofat

Functional Group (cm ⁻¹)	Standard Wav	venumber	Observed Frequency (cm ⁻¹)
Hydroxyl (O-H Stretch)	3400 – 3700	3360	- 3490
Methyl C-H (CH ₂ , CH ₃)	2920 - 2850	2920	-2852
Lipids/phospholipids (C=O ester)	1740 - 1750	1745	
Protein (collagen) (C=O amide I)	1650 - 1630	1651	

Table 2. FTIR interpretation of FDBB with 1 cc nanofat

Observ

Functional Group

(cm⁻¹)

Standard Wavenumber

Carboxylic acid/collagen (COO-	1450 - 1410	1402 - 1462
bending)		
Phosphate (PO ₄ ³⁻)	1030 - 1090 / 875 / 560 -	1032 - 1090 / 875 / 560
	600	-600

The FTIR analysis of FDBB combined with 2 cc of nanofat demonstrated a further increase in intensity for bands associated with organic components, suggesting an accumulation of lipids and proteins. A strong, broad OH stretch was observed at 3360–3490 cm⁻¹, attributed to water and polar groups in nanofat. C–H stretching bands at 2920 and 2852 cm⁻¹ were more prominent, indicating higher lipid content. Ester carbonyl (C=O) and amide I bands at 1745 cm⁻¹ and 1650–1638 cm⁻¹ respectively, confirmed protein and fat presence. Carboxylate bands were also evident at 1400–1460 cm⁻¹. Phosphate groups (PO₄³⁻) were still detectable at 1032–1090 cm⁻¹, 875 cm⁻¹, and 560–600 cm⁻¹, indicating the mineral structure was preserved, though possibly partially obscured by nanofat components.

Table 3. FTIR interpretation of FDBB with 2 cc nanofat

ctional Group -1)	Standard Wavenumber	Observed Frequency (cm ⁻¹)
Hydroxyl (O-H Stretch) Methyl C-H (CH ₂ , CH ₃)	3400 – 3700 2920 – 2850	3360 – 3490 2920 – 2852
Lipids/phospholipids (C=O ester) Protein (collagen) (C=O amide I)	1740 – 1750 1650 – 1630	1745 1650 – 1638
Carboxylic acid/collagen (COObending)	1450 – 1410	1400 – 1460
Phosphate (PO ₄ ³⁻)	1030 - 1090 / 875 / 560 - 600	1032 - 1090 / 875 / 560 - 600

The X-ray diffraction (XRD) analysis revealed differences in the crystallinity of the three FDBB groups. The sample with 1 cc nanofat exhibited a single broad peak with high intensity (350 cps) at $2\theta \approx 20^\circ$, indicating a semi-crystalline structure with low regularity, possibly representing collagen or biological protein domains. In the 2 cc nanofat group, the diffraction peak was still centered at $2\theta \approx 20^\circ$, but with lower intensity (216 cps), suggesting reduced crystallinity and a shift toward a more amorphous structure. In contrast, the control group (without nanofat) displayed a flat, broad diffraction pattern with the highest peak at only 133 cps, confirming a low-crystalline or amorphous structure.

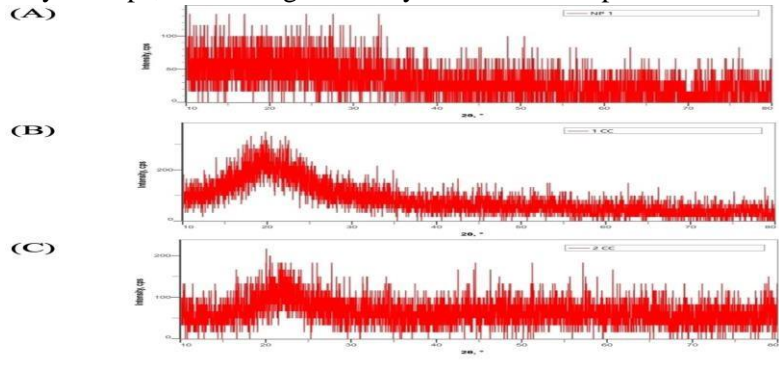


Figure 2. XRD Pattern Comparison. (A) FDBB Control (no nanofat), (B) FDBB + 1 cc nanofat, (C) FDBB + 2 cc nanofat

These findings indicate that the addition of 1 cc nanofat enhances the crystallinity of the FDBB scaffold, while 2 cc nanofat reduces this effect, returning the material toward an amorphous state.

DISCUSSION

Human bone is a natural biocomposite composed of cells embedded in a matrix containing both organic and inorganic components. The inorganic phase consists primarily of bone apatite, which includes phosphate (PO₄³⁻) and hydroxyl (OH) groups, while the organic phase is mainly composed of collagen proteins characterised by functional groups such as C–O–C, C–N, N–H, and O–H. ¹¹,18,19

FTIR analysis of freeze-dried bovine bone (FDBB) without nanofat revealed typical bone tissue functional groups. The broad peak between 3435–3786 cm⁻¹ corresponds to hydroxyl (–OH) stretching, likely arising from bound water and hydroxyl groups within hydroxyapatite (HA). Aliphatic C–H stretching bands at 2920 and 2854 cm⁻¹ indicated residual organic matter such as lipids or proteins. A carbonyl (C=O) band at 1745 cm⁻¹ suggested the presence of esters, while amide I at 1650 cm⁻¹ represented collagen. Carboxylate (COO⁻) vibrations were observed at 1400–1460 cm⁻¹. Phosphate bands—essential indicators of HA—were prominent at 1032–1090 cm⁻¹, 875 cm⁻¹, and 560–600 cm⁻¹, confirming the mineral bone structure.⁵,14

The addition of 1 cc and 2 cc nanofat to FDBB led to notable alterations in the FTIR spectrum. Increased intensity in the –OH band (3360–3490 cm⁻¹) reflected additional water and polar groups introduced by nanofat. The aliphatic C– H bands became more pronounced, consistent with a higher lipid content. Stronger C=O absorption at 1745 cm⁻¹ indicated the presence of triglycerides and phospholipids, while the amide I peak at 1651 cm⁻¹ suggested elevated protein levels. Similarly, increased COO⁻ intensity (1402–1462 cm⁻¹) pointed to enhanced fatty acid and protein contributions. Despite these organic additions, the phosphate bands remained visible, confirming preservation of HA mineral structure. ¹⁵

These findings indicate that nanofat supplementation successfully enhances protein and lipid content without disrupting the fundamental HA mineral structure. Nanofat, derived from adipose tissue, is rich in bioactive compounds including growth factors, fatty acids, and extracellular matrix proteins (Zuk et al., 2002). These organic components are pivotal in osteointegration processes, supporting cellular recruitment, bioactivity enhancement, and osteogenic differentiation. The presence of collagenrelated amide I and COO⁻ groups plays a critical role in osteoblast adhesion and proliferation and facilitates mineral deposition. 3,10

Furthermore, the lipid content of nanofat creates a microenvironment resembling native bone tissue, enhancing the biological compatibility of FDBB. Certain lipid structures have demonstrated pro-

regenerative effects, such as promoting angiogenesis and modulating local immune responses (Barba et al., 2013). However, excessive nanofat—as in the 2 cc group—may lead to dominance of organic signals, potentially interfering with HA's crystalline structure, which is crucial for mechanical strength. Achieving an optimal organic-inorganic ratio is thus vital to maintaining both bioactivity and biomechanical integrity. The X-ray diffraction (XRD) analysis further validated these observations. FDBB without nanofat displayed a flattened diffraction pattern with a maximum intensity of 133 cps, indicating a predominantly amorphous structure. This is consistent with the altered crystallinity commonly observed in freeze-dried bone biomaterials, which disrupt HA's natural lattice. ¹³

Upon addition of 1 cc nanofat, diffraction intensity markedly increased to 350 cps, with broader peaks indicative of a semi-crystalline structure. This suggests partial reorganisation of HA crystallinity, likely due to the interaction of nanofat- derived proteins and lipids with HA, stabilising the matrix and biologically mimicking mild annealing processes. In contrast, the 2 cc nanofat group exhibited reduced intensity (216 cps), although the 2θ peak remained at 20° , characteristic of HA. This reduction likely stems from excess organic material coating the mineral surface, hindering crystal growth and promoting a more amorphous state.

These results align with findings by Weinstein et al., who reported that lipid- protein interactions can disrupt crystal or membrane stability hydrophobic interference and local molecular environment modulation. Thus, while moderate nanofat enhances crystallinity, excessive amounts compromise crystal integrity. In summary, moderate nanofat supplementation (1 cc) promotes beneficial biomolecular interactions that restore HA crystallinity, whereas higher concentrations (2 cc) may hinder crystal development. Careful modulation of organic content is essential for optimising scaffold mechanical stability osteointegration potential. 12,13

This study is limited by its in vitro nature and lack of quantitative biochemical assays for protein and lipid content validation. The semi-quantitative FTIR and XRD interpretations provide essential insights but should be corroborated by complementary analyses such as thermogravimetric analysis (TGA) and scanning electron microscopy (SEM). Future studies should focus on in vivo evaluations, examining osteoconductivity, biocompatibility, and long-term mechanical stability of FDBB—nanofat scaffolds. Determining the optimal nanofat concentration for balancing bioactivity and structural integrity will also be essential for clinical applications.

CONCLUSIONS

This study demonstrates that the addition of nanofat, particularly at a volume of 1 cc, significantly enhances the chemical composition and crystallinity of freeze-dried bovine bone (FDBB) without compromising its essential mineral phase. The FTIR analysis revealed an increase in organic functional groups, such as amide and lipid bands, indicating improved bioactivity. Simultaneously, XRD data showed a transition towards a semi-crystalline structure, which may benefit mechanical stability and osteointegration. However, the incorporation of higher volumes, such as 2 cc, resulted in a reduction of crystallinity due to the masking effect of excessive organic content on hydroxyapatite surfaces.

DECLARATIONS

Ethics approval and consent to participate Not applicable.

Conflict interests

The authors declared no potential conflicts of interest with respect to the research, authorship, and/or publication of this article.

Funding

This research received no external funding.

REFERENCES

- Sandor, G. K., Kállai, I. Z., and Kocsis, L. 2014. Adipose Stem Cells Used to Reconstruct 13 Cases with Cranio-Maxillofacial Hard-Tissue Defects. sanSTEM CELLS Translational Medicine 3 (11): 1482–1493.https://doi.org/10.5966/sctm.2013-0173.
- Barba, M., Cicione, C., Bernardini, C., Michetti, F., 2. W. (2013).Adipose-Derived Lattanzi, Mesenchymal Cells for Bone Regereneration: State of the Art. BioMed Research International, 2013, 1-11. https://doi.org/10.1155/2013/416391
- Bonomi, F., Limido, E., Weinzierl, A., Ampofo, E., Harder, Y., Menger, M. D., & Laschke, M. W. Nanofat Improves Vascularization and Tissue Integration of Dermal Substitutes without Affecting Their Biocompatibility. FunctionalBiomaterials,2024;15(10),294. https://doi.org/10.3390/jfb15100294
- Carvalho, M. S., Cabral, J. M. S., da Silva, C. L., & Vashishth, D. Bone Matrix Non- Collagenous Proteins in Tissue Engineering: Creating New Bone by Mimicking the Extracellular Matrix. Polymers. 2024; 13(7), 1095. https://doi.org/10.3390/polym13071095
- Ding, P., Lu, E., Li, G., Sun, Y., Yang, W., & Zhao, Z. Research Progress on Preparation, Mechanism, and Clinical Application of Nanofat. Journal of Burn & Research, 2020; 43(5), 1140-1144. https://doi.org/10.1093/jbcr/irab250
- Dorozhkin, S. V. Bioceramics of calcium

- orthophosphates. Biomaterials, 2010; 31(7), 1465–1485. https://doi.org/10.1016/j.biomaterials.2009.11.050
- Han, Y., Li, X., Zhang, Y., Han, Y., Chang, F., & Ding, J. (2019). Mesenchymal Stem Cells for Regenerative Medicine. Cells, 8(8),https://doi.org/10.3390/cells8080886 Haugen, H. J., Lyngstadaas, S. P., Rossi, F., & Perale, G. Bone grafts: which is theideal biomaterial? Journal of Clinical Periodontology,2019 46(S21), https://doi.org/10.1111/jcpe.13058
- Hong, M.-H., Lee, J. H., Jung, H. S., Shin, H., & Shin, H. Biomineralization of bone tissue: calcium phosphatebased inorganics in collagen fibrillar organic matrices. BiomaterialsResearch,2020;26(1). https://doi.org/10.1186/s40824-022-00288-0
- LeGeros. R. Z. Calcium Phosphate-Based Osteoinductive Materials. Chemical Reviews, 2008; 108(11), 4742–4753. https://doi.org/10.1021/cr800427g
- 10. Lin, X., Patil, S., Gao, Y.-G., & Qian, A. The Bone Extracellular Matrix in Bone Formation and Regeneration. **Frontiers** in *Pharmacology*, 2020; 11. https://doi.org/10.3389/fphar.20 20.00757
- 11. Liu, Q., Huang, S., Matinlinna, J. P., Chen, Z., & Pan, H. Insight into Biological Apatite: Physiochemical Properties and Preparation Approaches. BioMed Research International, 2013. https://doi.org/10.1155/2013/929748
- 12. Miri, Z., Haugen, H. J., Loca, D., Rossi, F., Perale, G., Moghanian, A., & Ma, Q. Review on the strategies to improve the mechanical strength of highly porous bone bioceramic scaffolds. Journal of the European Ceramic Society, 2024;44(1), 23–42. https://doi.org/10.1016/j.jeurceramsoc.2023.09.003
- 13. Mishchenko, O., Yanovska, A., Kosinov. Maksymov, D., Moskalenko, R., Ramanavicius, A., & Pogorielov, M. Synthetic Calcium–Phosphate Materials Bone Grafting. Polymers, 2023; for 15(18),3822.https://doi.org/10.3390/polym15183822
- 14. Müller, L., Conforto, E., Caillard, D., & Müller, F. A. Biomimetic apatite coatings— Carbonate substitution preferred growth orientation. Biomolecular Engineering, 2007; 24(5), 462–466. https://doi.org/10.1016/j.bioeng.2007.07.011
- 15. Rajendran, A. K., Anthraper, M. S. J., Hwang, N. S., & Rangasamy, J. Osteogenesis and angiogenesis promoting bioactive ceramics. Materials Science and Engineering: R: Reports, 2024; 159. https://doi.org/10.1016/j.mser.2024.100801
- 16. Tonnard, P., Verpaele, A., Peeters, G., Hamdi, M., Cornelissen, M., & Declercq, H. Nanofat Grafting. Plastic and Reconstructive Surgery, 2013;132(4), 1017-1026. https://doi.org/10.1097/PRS.0b013e31829fe1b0